

# Chain Compounds Based on Tetranuclear Basic Copper(II) Carboxylate Clusters and Quadruple Zwitterionic Linkers: Structures and Magnetic Properties

Xiu-Mei Zhang,<sup>[a]</sup> Yan-Qin Wang,<sup>[a]</sup> and En-Qing Gao<sup>\*[a]</sup>

**Keywords:** Zwitterions / Copper / Magnetic properties / Coordination polymers / Carboxylate ligands

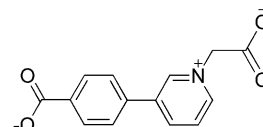
Two Cu<sup>II</sup> complexes with the new zwitterionic ligand 1-carboxymethylpyridinio-3-benzoate (**L**), [Cu<sub>4</sub>L<sub>4</sub>(OH)<sub>2</sub>](ClO<sub>4</sub>)<sub>2</sub>·8H<sub>2</sub>O (**1**) and [Cu<sub>4</sub>L<sub>4</sub>(OH)<sub>2</sub>]Cl<sub>2</sub>·8H<sub>2</sub>O (**2**), have been synthesized and characterized crystallographically and magnetically. The two compounds contain isostructural chains, in which the anionic basic copper(II) carboxylate clusters

[Cu<sub>4</sub>(μ<sub>3</sub>-OH)<sub>2</sub>(RCOO)<sub>8</sub>]<sup>2-</sup> are quadruply interlinked by cationic organic spacers. Magnetic analyses using a tetranuclear model indicate that antiferromagnetic interactions between neighboring copper(II) ions are operative through the double hydroxo bridges and the mixed hydroxo/carboxylato bridges.

## Introduction

Polynuclear and polymeric copper(II) coordination compounds with carboxylato ligands have attracted much attention for decades.<sup>[1,2d]</sup> For monocarboxylato ligands, the most common structural motif is the dinuclear “paddlewheel” [Cu<sub>2</sub>(RCOO)<sub>4</sub>] core, which has been subjected to many magnetostructural studies.<sup>[3]</sup> The core also serves as the secondary building unit in many porous metal–organic frameworks with di- or tricarboxylato ligands.<sup>[2]</sup> The structural diversity of copper(II) carboxylate systems is much enhanced by the incorporation of various coligands, either terminal or bridging. For instance, the co-ordination of short bridging ligands such as hydroxo,<sup>[4]</sup> alkoxo,<sup>[5]</sup> and azido<sup>[6]</sup> with carboxylate has led to a great variety of discrete polynuclear molecules or extended coordination polymers with interesting features relevant to magnetostructural correlations, bioinorganic modeling, or molecular magnets. The majority of the carboxylato ligands [RCOOH or R(COOH)<sub>n</sub> (*n* = 2 or 3)] used so far bear neutral R groups, and the carboxylic group is deprotonated to give anionic ligands upon coordination. The carboxylato ligands that bear positive R groups (e.g., Me<sub>3</sub>N<sup>+</sup>CH<sub>2</sub>-, *N*-methylenepyridinium) have received less attention.<sup>[7–9]</sup> The zwitterionic ligands may lead to new coordination structures with Cu<sup>II</sup>.<sup>[10]</sup> Recently, we have demonstrated that the combination of zwitterionic dicarboxylato ligands and azido coligands could easily form novel coordination networks with mixed carboxylato and azido bridges, which exhibit inter-

esting magnetic features.<sup>[11]</sup> In this article, we report the synthesis, structure, and magnetic properties of two Cu<sup>II</sup> compounds with a new zwitterionic dicarboxylato ligand, 1-carboxymethyl-3-(4-carboxyphenyl)pyridinium (**L**, Scheme 1). The compounds are of formula [Cu<sub>4</sub>(OH)<sub>2</sub>L<sub>4</sub>]-X<sub>2</sub>·8H<sub>2</sub>O (X = ClO<sub>4</sub><sup>-</sup>, **1**; X = Cl<sup>-</sup>, **2**), and are one-dimensional coordination polymers based on the unprecedented anionic tetranuclear “basic copper(II) carboxylate” cluster [Cu<sub>4</sub>(μ<sub>3</sub>-OH)<sub>2</sub>(RCOO)<sub>8</sub>]<sup>2-</sup>, which is quadruply interlinked by cationic organic spacers.



Scheme 1. Chemical structure of **L**.

## Results and Discussion

### Description of the Structures

Although crystallized in different space groups, both **1** and **2** are 1D chain compounds that feature tetracopper(II) clusters linked by **L** ligands. The asymmetric unit contains two unique Cu atoms (Cu1 and Cu2), a hydroxo anion, two unique **L** ligands, a perchlorate (**1**) or chloride (**2**) anion, and some solvent molecules. Selected bond lengths and angles are listed in Table 1.

The tetracopper cluster is depicted in Figure 1 (a). It contains a centrosymmetric [Cu<sub>4</sub>(OH)<sub>2</sub>]<sup>6+</sup> core, in which four Cu<sup>II</sup> atoms are linked by two equivalent μ<sub>3</sub>-OH bridges to form a planar rhombus. The geometry can also be de-

[a] Shanghai Key Laboratory of Green Chemistry and Chemical Processes, Department of Chemistry, East China Normal University, Shanghai 200062, China  
Fax: +86-21-62233404  
E-mail: eqgao@chem.ecnu.edu.cn

Table 1. Selected bond lengths [Å] and angles [°] for compounds **1** and **2**.<sup>[a]</sup>

	<b>1</b>	<b>2</b>
Cu1–O5A	1.929(2)	1.944(2)
Cu1–O9	1.958(2)	1.962(2)
Cu1–O4A	2.027(2)	2.011(2)
Cu1–O1	2.039(2)	2.026(2)
Cu1–O7A	2.159(3)	2.183(2)
Cu2–O2	1.938(2)	1.942(2)
Cu2–O3A	1.974(2)	1.960(2)
Cu2–O9	1.983(2)	1.982(2)
Cu2–O9A	1.986(2)	1.985(2)
Cu2–O8	2.237(2)	2.211(2)
O5A–Cu1–O9	169.95(10)	170.04(10)
O5A–Cu1–O4A	85.93(10)	85.21(9)
O9–Cu1–O4A	90.17(10)	90.52(9)
O5A–Cu1–O1	88.69(10)	89.97(9)
O9–Cu1–O1	92.86(10)	92.11(9)
O4A–Cu1–O1	165.42(11)	166.14(10)
O5A–Cu1–O7A	93.13(10)	91.33(9)
O9–Cu1–O7A	96.84(10)	98.48(10)
O4A–Cu1–O7A	105.46(11)	105.32(10)
O1–Cu1–O7A	88.34(11)	87.75(9)
O2–Cu2–O3A	89.78(10)	89.53(9)
O2–Cu2–O9	95.13(10)	94.89(9)
O3A–Cu2–O9	165.78(10)	166.07(10)
O2–Cu2–O9A	171.83(10)	171.95(10)
O3A–Cu2–O9A	93.85(10)	92.92(9)
O9–Cu2–O9A	79.67(10)	81.00(10)
O2–Cu2–O8	85.65(10)	86.59(10)
O3A–Cu2–O8	96.45(10)	96.38(10)
O9–Cu2–O8	97.22(10)	97.06(10)
O9A–Cu2–O8	101.18(9)	100.74(9)
Cu1–O9–Cu2	117.98(12)	118.47(12)
Cu1–O9–Cu2A	110.79(12)	110.67(11)
Cu2–O9–Cu2A	100.33(10)	99.00(10)

[a] Symmetry code: A:  $-x, -y, -z$ .

scribed as two  $\text{Cu}_3\text{O}$  trigonal pyramids that share the basal edge defined by two centrosymmetry-related and double hydroxo-bridged Cu2 atoms, with  $\text{Cu2}\cdots\text{Cu2A}$  3.048(1) Å for **1** and 3.017(1) Å for **2**. The M–O–M angles around the  $\mu_3$ -OH (O9) range from 99.0 to 118.5°. The sum (329° for **1** and 328° for **2**) of the three angles around each  $\mu_3$ -OH is in good agreement with the tetrahedral environment of the oxygen atom, and the oxygen atom is displaced out of the  $\text{Cu}_3$  plane by 0.65 Å for **1** and 0.66 Å for **2**, thereby defining a rather flat pyramidal shape for  $\text{Cu}_3\text{O}$ . The tetranuclear  $[\text{Cu}_4(\mu_3\text{-OH})_2]^{6+}$  core is reinforced by six carboxylato bridges in the *syn-syn* coordination mode. There are two different bridging fashions between Cu1 and Cu2 sites. One is the double-bridging motif that contains a  $\mu_3$ -hydroxo and a carboxylato (O1–C–O2), with  $\text{Cu1}\cdots\text{Cu2}$  3.378(2) Å for **1** and 3.389(1) Å for **2**; the other is the triple-bridging motif consisting of a  $\mu_3$ -hydroxo and two carboxylato ligands (O3–C–O4 and O7–C–O8), with shorter  $\text{Cu1}\cdots\text{Cu2A}$  distances of 3.246(2) Å for **1** and 3.246(1) Å for **2**. The resulting  $[\text{Cu}_4(\mu_3\text{-OH})_2(\text{RCOO})_6]$  cluster is reminiscent of the well-known clusters  $[\text{M}_4(\mu_3\text{-O})_2(\text{RCOO})_6]^{n+}$  ( $n = 0-2$ , M = Mn, Fe, Cr), which have been extensively studied for decades due to their great relevance to biological systems and magnetic materials.<sup>[12]</sup> Besides the difference in

the  $\mu_3$  bridge ( $\text{OH}^-$  vs.  $\text{O}^{2-}$ ), the major difference is that the previous clusters contain high-valence metals (mixed-valent  $\text{M}^{\text{II}}\text{M}^{\text{III}}$  or homovalent  $\text{M}^{\text{III}}$ ).

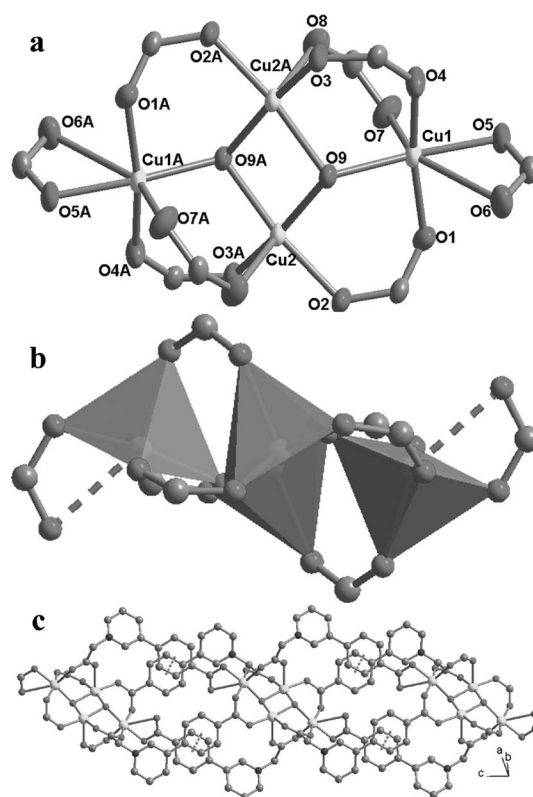


Figure 1. (a) The tetranuclear cluster in **1** and **2** (thermal ellipsoids are drawn at 30% probability). (b) The view showing the arrangement of the coordination polyhedra in the cluster. (c) The 1D chain constructed from the clusters.

The coordination geometry of  $\text{Cu}^{\text{II}}$  in the cluster is worth further clarification from the viewpoints of coordination chemistry and magnetochemistry. The Cu2 ion resides in a square-pyramidal environment. The basal plane is defined by two  $\mu_3$ -hydroxo oxygen atoms (O9 and O9A) and two carboxylato oxygen atoms (O2 and O3), and a third carboxylato oxygen (O8) occupies the apical position. The basal Cu–O distances (1.94–1.99 Å) are significantly shorter than the apical ones (ca. 2.24 Å). The basal atoms deviate from their mean plane by less than 0.0555(16) Å, and Cu2 is out of the mean basal plane by 0.171(1) Å in **1** or 0.173(1) Å in **2**. The geometry around Cu1 is also square pyramidal, also with a carboxylato oxygen (O7) at the apical position, but the basal plane is completed by a  $\mu_3$ -hydroxo oxygen (O9) and three carboxylato oxygen atoms (O1, O4, and O5). Again, the basal Cu–O distances (1.93–2.04 Å) are shorter than the apical ones (ca. 2.16 Å). The deviations of the basal atoms from the basal mean plane are less than 0.0425(13) Å, and Cu1 is at 0.2053(13) Å (**1**) or 0.1975(12) Å (**2**) above the basal plane. The basal planes of Cu1 and Cu2 have a dihedral angle of 48.00(9)° in **1** or 48.12(8)° in **2**. Notably, the O7–C–O8 carboxylato bridge adopts the apical–apical disposition in Figure 1 (b) (i.e., the oxygen atoms reside at the apical positions of the two  $\text{Cu}^{\text{II}}$

ions it links), whereas the O1–C–O2 and O3–C–O4 carboxylato bridges are disposed in the basal–basal fashion. The  $\mu_3$ -OH bridge lies in the basal planes of all the  $\text{Cu}^{\text{II}}$  ions it binds. These features are of particular relevance to the magnetic properties. It should be noted that Cu1 is weakly coordinated by O6 from the O5–C–O6 carboxylato, with a rather long Cu–O distance of 2.61 Å. If this is included, the O5–C–O6 carboxylato binds Cu1 in an asymmetric chelating mode, and the geometry around Cu1 may be described as a highly distorted octahedron. Taking into account the semichelating carboxylato ligands, the cluster has a stoichiometry of  $[\text{Cu}_4(\mu_3\text{-OH})_2(\text{RCOO})_8]^{2-}$ . For comparison, the previous  $[\text{M}_4(\mu_3\text{-O})_2(\text{RCOO})_6]^{n+}$  ( $n = 0\text{--}2$ ,  $\text{M} = \text{Mn}, \text{Fe}, \text{Cr}$ ) clusters<sup>[12]</sup> have non-carboxylato ligands (usually, the chelating 2,2'-bipyridine and its analogues) to complete the coordination geometry. To the best of our knowledge, the anionic “basic carboxylate”  $\text{Cu}^{\text{II}}_4$  motif in **1** and **2** is unprecedented. Two different “basic carboxylate”  $\text{Cu}^{\text{II}}_4$  clusters have been reported elsewhere. One is  $[\text{Cu}(\text{oct})_6(\text{OH})_2(4\text{-apy})_2]^{13}$  (**3**; oct = octanoate, 4-apy = 4-aminopyridine), which contains the neutral  $[\text{Cu}_4(\mu_3\text{-OH})_2(\text{RCOO})_6]$  motif with terminal N donors (4-apy). An interesting difference is that the apical–apical *syn*–*syn* carboxylato bridge in **1** and **2** is replaced by a monodentate carboxylato bridge in **3**, which uses a  $\mu_2$ -O atom to bridge two metal ions (also in the apical–apical disposition). The other basic tetracopper carboxylato is  $[\text{Cu}_4(\text{tfc})_6(\text{OH})_2(\text{quin})_4]^{14}$  (**4**; tfc = trifluoroacetate, quin = quinoline), which also contains the neutral  $[\text{Cu}_4(\mu_3\text{-OH})_2(\text{RCOO})_6]$  motif with terminal N donors (quin). However, the bridging network in **4** is different from those in **1–3**. In **4**, there are two nonbridging monodentate carboxylato groups that bind Cu2 atoms. The neighboring Cu1 and Cu2 atoms are either triply bridged by two carboxylato bridges in the basal–apical disposition and a  $\mu_3$ -OH, or singly bridged by  $\mu_3$ -OH. Clearly, the formation of the anionic  $[\text{Cu}_4(\mu_3\text{-OH})_2(\text{RCOO})_8]^{2-}$  clusters in **1** and **2** is facilitated by the zwitterionic carboxylato ligand.

The tetranuclear cluster has eight peripheral carboxylato groups (two in the pseudochelating mode and six in the *syn*–*syn* bridging mode) from different **L** ligands. The flexible methylene group and the 3-substituted pyridyl group in the organic ligand collaborate to define a twisted and bent bridging conformation for the whole ligand. The ligands in such conformations serve as quaternate bridges to link the clusters into an infinite chain along the crystallographic *c* (**1**) or *a* (**2**) direction. The unusual chain looks like a thick rope in which four strands join at the clusters. The four ligands between two neighboring clusters are arranged in pairs by  $\pi$ – $\pi$  interactions (Figure 1, c). The benzene ring of a ligand is nearly parallel to the benzene ring of a crystallographically independent ligand, with evident face-to-face overlap. For **1**, the dihedral angle between the interacting rings is 5.0°, and the center-to-center distance and the average atom-to-plane distance are 3.59 and 3.44 Å, respectively. The parameters for **2** are similar. In both compounds, the chains are packed in parallel, and the perchlorate (or chloride) anions and lattice water molecules occupy the interchain spaces.

## Magnetic Properties

The magnetic susceptibilities ( $\chi$ ) of compounds **1** and **2** were measured on crystalline samples under 1 kOe in the range of 2–300 K and are shown as  $\chi T$  and  $\chi$  versus  $T$  plots in Figures 2 and 3, respectively. The two compounds show similar temperature-dependent behaviors. The  $\chi T$  values per tetracopper cluster at 300 K are about 1.64  $\text{emu K mol}^{-1}$ , comparable with the spin-only value (1.50  $\text{emu K mol}^{-1}$  from  $g = 2.00$ ) expected for four magnetically isolated  $\text{Cu}^{\text{II}}$  ions. As the temperature is lowered, the  $\chi T$  value decreases continuously, whereas the  $\chi$  value first increases to a maximum at 6 K for **1** and 7 K for **2** and then decreases rapidly towards zero at lower temperature. The data above 50 K follow the Curie–Weiss law with  $C = 1.85 \text{ emu K mol}^{-1}$  and  $\theta = -41.6 \text{ K}$  for **1**, and  $C = 1.86 \text{ emu K mol}^{-1}$  and  $\theta = -38.2 \text{ K}$  for **2**. The above characteristics clearly suggest overall antiferromagnetic interactions between  $\text{Cu}^{\text{II}}$  ions in these compounds.

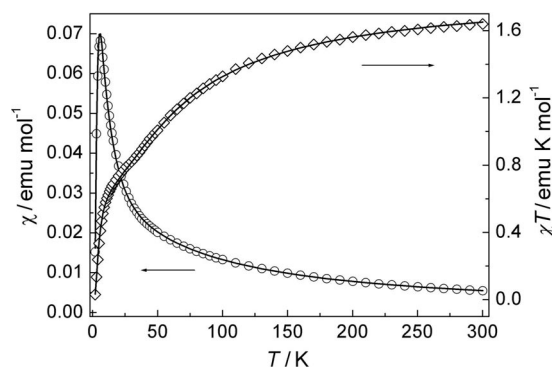


Figure 2. Thermal variations of  $\chi$  and  $\chi T$  for **1** under 1 kOe. The solid lines represent the best fit to the van Vleck equation.

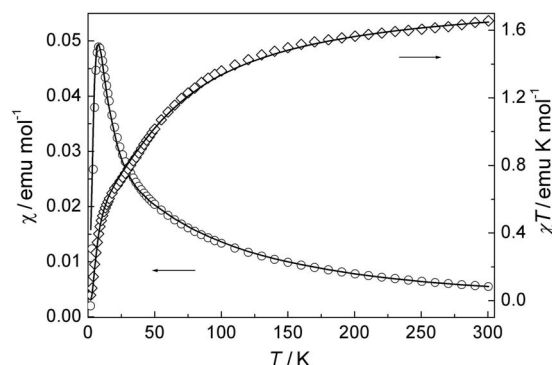
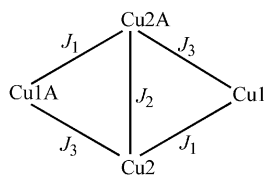


Figure 3. Thermal variations of  $\chi$  and  $\chi T$  for **2** under 1 kOe. The solid lines represent the best fit to the van Vleck equation.

Based on the structural data, there are three different bridging motifs between adjacent  $\text{Cu}^{\text{II}}$  ions in the tetranuclear rhombic cluster:  $\text{Cu}_2(\text{OH})_2\text{Cu}_2\text{A}$ ,  $\text{Cu}_1(\text{OH})(\text{RCOO})\text{Cu}_2$ , and  $\text{Cu}_1(\text{OH})(\text{RCOO})_2\text{Cu}_2\text{A}$ . The superexchange scheme can be represented as shown in Scheme 2.



Scheme 2. The coupling scheme of the cluster.

The corresponding spin Hamiltonian is  $H = -2J_1(\mathbf{S}_{2A}\mathbf{S}_{1A} + \mathbf{S}_2\mathbf{S}_1) - 2J_2\mathbf{S}_{2A}\mathbf{S}_2 - 2J_3(\mathbf{S}_{2A}\mathbf{S}_1 + \mathbf{S}_2\mathbf{S}_{1A})$ . The energy matrix can be solved to give the following six energy levels with the total spin ( $S$ ) of 0, 1, and 2.<sup>[15]</sup>

$$E_1 = -J_1 - J_2/2 - J_3, S = 2$$

$$E_2 = J_1 - J_2/2 + J_3, S = 1$$

$$E_3 = J_2/2 + [J_2^2 + (J_3 - J_1)^2]^{1/2}, S = 1$$

$$E_4 = J_2/2 - [J_2^2 + (J_3 - J_1)^2]^{1/2}, S = 1$$

$$E_5 = J_1 + J_3 + J_2/2 + [4(J_1^2 + J_3^2) + J_2^2 - 4J_1J_3 - 2J_1J_2]^{1/2}, S = 0$$

$$E_6 = J_1 + J_3 + J_2/2 - [4(J_1^2 + J_3^2) + J_2^2 - 4J_1J_3 - 2J_1J_2]^{1/2}, S = 0$$

Applying the energy eigenvalues to the van Vleck equation yields the following analytical expression of the magnetic susceptibility; see Equation (1).

$$\chi = \frac{2N\beta^2 g^2 A}{kT} \left( \frac{1}{B} \right) \quad (1)$$

$$A = 5\exp(-E_1/kT) + \exp(-E_2/kT) + \exp(-E_3/kT) + \exp(-E_4/kT) \text{ and } B = 5\exp(-E_1/kT) + 3\exp(-E_2/kT) + 3\exp(-E_3/kT) + 3\exp(-E_4/kT) + \exp(-E_5/kT) + \exp(-E_6/kT)$$

The experimental data for **1** and **2** can be simulated by the above expression. The best-fit parameters are  $J_1 = -16.2 \text{ cm}^{-1}$ ,  $J_2 = -27.9 \text{ cm}^{-1}$ ,  $J_3 = -13.8 \text{ cm}^{-1}$ , and  $g = 2.20$  for **1**; and  $J_1 = -15.3 \text{ cm}^{-1}$ ,  $J_2 = -25.8 \text{ cm}^{-1}$ ,  $J_3 = -14.8 \text{ cm}^{-1}$ , and  $g = 2.21$  for **2**.

The  $J_2$  values suggest a moderate antiferromagnetic interaction through the double hydroxo bridge between Cu2 and Cu2A. It is well known that the interaction in the double-hydroxo-bridged Cu<sup>II</sup> systems is sensitive to the Cu–O–Cu angle. For systems with large bridging angles ( $>97.5^\circ$ ), the interaction is antiferromagnetic and the magnitude increases as the angle increases.<sup>[15,16]</sup> The two present isostructural compounds follow this trend well: **1** has a larger Cu2–O–Cu2A angle [ $100.3(1)^\circ$ ] than **2** [ $99.0(1)^\circ$ ], and hence exhibits a stronger antiferromagnetic interaction.

The  $J_1$  and  $J_3$  values suggest the interactions through the mixed triple [(OH)(RCOO)<sub>2</sub>] and double [(OH)(RCOO)] bridges are also antiferromagnetic. As has been noted, one of the carboxylato ligands in the triple-bridging motif adopts an apical–apical disposition between Cu<sup>II</sup> ions, whereas the other bridges are in the basal–basal dispositions. Since the magnetic orbital for Cu<sup>II</sup> in axially elongated square-pyramidal fields is of the  $d_{x^2-y^2}$  type and is mainly delocalized towards the basal ligands, the magnetic coupling through the apical–apical bridge should be negligibly small.<sup>[17]</sup> Therefore, the apical–apical carboxylato path-

way in the triple-bridging motif can be neglected from the magnetic viewpoint, and both the triple and double motifs have a hydroxo and a carboxylato as effective exchange pathways. However, the incorporation of the apical–apical carboxylato may be responsible for the decreased Cu–O–Cu angle and Cu...Cu distance in the triple motif with respect to those in the double motif, and hence may influence magnetic coupling in an indirect way. The larger  $J_1$  parameters may be assigned to the double motif, which has a larger Cu–O–Cu angle, but the assignment should be regarded as being very tentative because the  $J_1$  and  $J_3$  values are very close to each other, especially for **2**.

The isothermal magnetization behaviors of **1** and **2** were measured from 0 to 50 kOe at 2 K (Figure 4). Upon applying the field up to 25 kOe, the magnetization for both compounds increases slowly and linearly, as expected for antiferromagnetic coupled systems with the  $S = 0$  ground state. A further increase of the field up to 50 kOe leads to a more and more rapid increase in magnetization. This behavior may be explained based on the Zeeman effect in the low-lying excited states. According to energy expressions and the  $J_1$ ,  $J_2$ , and  $J_3$  values obtained above, the cluster has the first excited state with  $S = 1$  at only several  $\text{cm}^{-1}$  (ca.  $6.4 \text{ cm}^{-1}$  for **1** and about  $8.5 \text{ cm}^{-1}$  for **2**) above the  $S = 0$  ground state. The Zeeman effect does not operate on the  $S = 0$  states but splits the  $S = 1$  state (Figure 5). As the field increases to a certain value, the crossover between the ground state and the  $M_S = -1$  ( $M_S$  is the magnetic quantum number of the spin state) component of the excited state occurs. The magnetization rise at higher field may be due to the rapidly increased population of the  $M_S = -1$  level as the field approaches the crossover point. A similar phenomenon has been documented for a trinuclear Mn<sup>II</sup> system and a tetranuclear Ni<sup>II</sup> system.<sup>[18]</sup> The observation that magnetization of **1** increases more rapidly than that of **2** is consistent with the smaller zero-field gap between the ground and first excited states in **1**. The smaller energy gap means that the crossover occurs at a lower field.

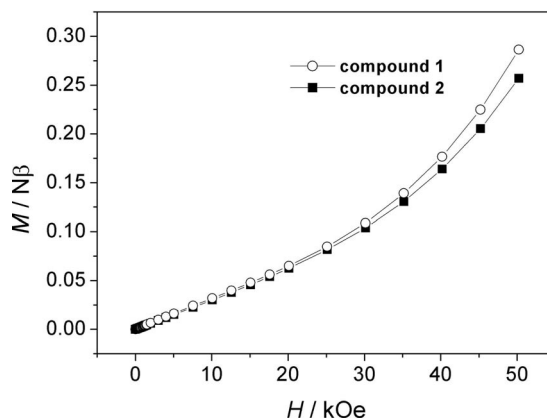


Figure 4. Field-dependent isothermal magnetization curves for compounds **1** and **2** at 2 K (the solid lines are only a guide for the eye).



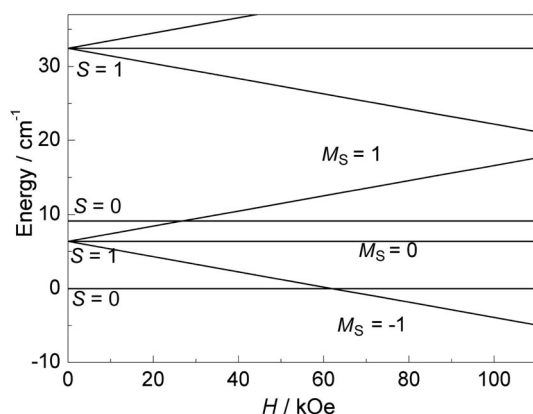


Figure 5. Energy levels of the low-lying spin states under external field, calculated according to the best-fit  $J$  and  $g$  values for **1** (see the text).

## Conclusion

We have described two 1D Cu<sup>II</sup> coordination polymers derived from the new zwitterionic dicarboxylate ligand 1-carboxymethyl-4-pyridinio-3-benzoate. The compounds contain the unprecedented anionic basic copper(II) carboxylate clusters of formula  $[\text{Cu}_4(\text{OH})_2(\text{RCOO})_8]^{2-}$ , which are quadruply interlinked by cationic pyridinium moieties. Magnetic investigations on the compounds revealed antiferromagnetic intra-tetramer interaction through the mixed hydroxo and carboxylato bridges.

## Experimental Section

**Materials and Physical Measurements:** All the solvents and reagents for synthesis were commercially available and used as received. The ligand HL was synthesized according to the literature methods for similar compounds.<sup>[19]</sup> Infrared spectra were recorded with a NEXUS 670 FTIR spectrometer using KBr pellets. Elemental analysis was carried out with an Elementar Vario El III elemental analyzer. Temperature- and field-dependent magnetic measurements were carried out with a Quantum Design SQUID MPMS-5 magnetometer. Diamagnetic corrections were made with Pascal's constants.

**$[\text{Cu}_4(\text{OH})_2\text{L}_4](\text{ClO}_4)_2 \cdot 8\text{H}_2\text{O}$  (**1**):** In a test tube, a solution of HL (0.10 mmol, 0.026 g) and  $\text{Cu}(\text{ClO}_4)_2 \cdot 6\text{H}_2\text{O}$  (0.10 mmol, 0.037 g) in methanol/water (1:1, 5 mL) was layered carefully with methanol/water (1:1, 3 mL) and then a solution of  $\text{HCOONa}$  (0.5 mmol, 0.034 g) in methanol (10 mL). The tube was sealed and left undisturbed at room temperature. X-ray-quality green block crystals appeared five days later. Yield 0.026 g, 62% based on  $\text{Cu}(\text{ClO}_4)_2 \cdot 6\text{H}_2\text{O}$ .  $\text{C}_{56}\text{H}_{58}\text{Cl}_2\text{Cu}_4\text{N}_4\text{O}_{34}$  (1651.95): calcd. C 40.61, H 3.53, N 3.38; found C 41.03, H 3.90, N 3.20. IR (KBr):  $\tilde{\nu}$  = 3520 (br), 3083 (w), 1646 (s), 1593 (m), 1398 (s), 1102 (s), 784 (m), 754 (m), 623 (m)  $\text{cm}^{-1}$ .

**$[\text{Cu}_4(\text{OH})_2\text{L}_4]\text{Cl}_2 \cdot 8\text{H}_2\text{O}$  (**2**):** The compound was prepared as green block crystals by the procedure described above for **1** except that copper perchlorate hexahydrate was replaced by copper chloride dihydrate. Yield 0.022 g, 58% based on  $\text{CuCl}_2 \cdot 2\text{H}_2\text{O}$ .  $\text{C}_{56}\text{H}_{58}\text{Cl}_2\text{Cu}_4\text{N}_4\text{O}_{26}$  (1523.99): calcd. C 44.01, H 3.83, N 3.67; found C 43.89, H 4.11, N 3.36. IR (KBr):  $\tilde{\nu}$  = 3370 (br), 3066 (w),

1642 (s), 1599 (w), 1401 (s), 1311 (m), 784 (w), 754 (w), 720 (w), 623 (w)  $\text{cm}^{-1}$ .

**Crystal Data Collection and Refinement:** Diffraction intensity data were collected at 293 K with a Bruker APEX II diffractometer equipped with a CCD area detector and graphite-monochromated Mo- $K_\alpha$  radiation ( $\lambda$  = 0.71073 Å). Empirical absorption corrections were applied using the SADABS program.<sup>[20]</sup> The structures were solved by the direct method and refined by the full-matrix least-squares method on  $F^2$ , with all non-hydrogen atoms refined with anisotropic thermal parameters.<sup>[21,22]</sup> The hydrogen atoms attached to carbon atoms were placed in calculated positions and refined using the riding model, and the hydrogen atoms of the hydroxo groups were located from the difference maps. The hydrogen atoms for the lattice water molecules could not be located due to the limited quality of the datasets. Pertinent crystallographic data and structure refinement parameters are summarized in Table 2.

Table 2. Crystal data and structure refinement parameters for compounds **1** and **2**.

	<b>1</b>	<b>2</b>
Formula	$\text{C}_{56}\text{H}_{58}\text{Cl}_2\text{Cu}_4\text{N}_4\text{O}_{34}$	$\text{C}_{56}\text{H}_{58}\text{Cl}_2\text{Cu}_4\text{N}_4\text{O}_{26}$
$M_r$	1656.12	1528.18
$T$ [K]	296	296
Crystal system	triclinic	monoclinic
Space group	$P\bar{1}$	$P2_1/c$
$a$ [Å]	10.7400(2)	13.9746(13)
$b$ [Å]	10.9397(2)	14.9708(14)
$c$ [Å]	13.9761(3)	14.3454(13)
$\alpha$ [°]	83.2860(10)	90
$\beta$ [°]	74.8080(10)	97.5570(10)
$\gamma$ [°]	81.6720(10)	90
$V$ [Å <sup>3</sup> ]	1562.62(5)	2975.1(5)
$Z$	1	4
$D_{\text{calcd.}}$ [g cm <sup>-3</sup> ]	1.760	1.692
$\mu$ [mm <sup>-1</sup> ]	1.532	1.591
Reflections collected	17408	18349
Unique reflections ( $R_{\text{int}}$ )	6088 (0.0260)	6736 (0.0371)
$R_1$ [ $I > 2\sigma(I)$ ]	0.0412	0.0425
$wR_2$ (all data)	0.1198	0.1196
GO $F$	1.039	1.058

CCDC-754932 (for **1**) and -754933 (for **2**) contain the supplementary crystallographic data for this paper. These data can be obtained free of charge from The Cambridge Crystallographic Data Centre via [www.ccdc.cam.ac.uk/data\\_request/cif](http://www.ccdc.cam.ac.uk/data_request/cif).

## Acknowledgments

We are thankful for the financial support from the Natural Science Foundation of China (20771038) and Shanghai Leading Academic Discipline Project (B409).

- [1] a) L. Gutierrez, G. Alzuet, J. A. Real, J. Cano, J. Borrás, A. Castiñeiras, *Eur. J. Inorg. Chem.* **2002**, 2094–2102; b) W. Mazurek, B. J. Kennedy, K. S. Murray, M. J. O'Connor, J. R. Rodgers, I. M. R. Snow, A. G. Wedd, P. R. Zwack, *Inorg. Chem.* **1985**, 24, 3258–3264; c) M. Lakshminarayanan, S. K. Tiwary, A. R. Chakravarty, *Inorg. Chem.* **1995**, 34, 5091–5093; d) S. Youngme, C. Chailuecha, G. A. van Albada, C. Pakawatchai, N. Chaichit, J. Reedijk, *Inorg. Chim. Acta* **2004**, 357, 2532–2542; e) A. Mukherjee, M. K. Saha, M. Nethaji, A. R. Chakravarty, *Polyhedron* **2004**, 23, 2177–2182.
- [2] a) O. M. Yaghi, M. O'Keefe, N. W. Ockwig, H. K. Chae, M. Eddaoudi, J. Kim, *Nature* **2003**, 423, 705–714; b) H. Furukawa,

- J. Kim, N. W. Ockwig, M. O'Keeffe, O. M. Yaghi, *J. Am. Chem. Soc.* **2008**, *130*, 11650–11661; c) S. K. Ghosh, S. Bureekaew, S. Kitagawa, *Angew. Chem. Int. Ed.* **2008**, *47*, 3403–3406; d) D. Tanaka, S. Horike, S. Kitagawa, M. Ohba, M. Hasegawa, Y. Ozawa, K. Toriumi, *Chem. Commun.* **2007**, 3142–3144.
- [3] a) Z. Deutsch, J. M. Rubin-Preminger, J. Bernstein, J. Y. Becker, *CrystEngComm* **2006**, *8*, 41–50; b) T. Da Ros, M. Prato, D. M. Guldi, M. Ruzzi, L. Pasimeni, *Chem. Eur. J.* **2001**, *7*, 816–827; c) M. J. Prakash, Y. Zou, S. Hong, M. Park, N. Bui, G. H. Seong, M. S. Lah, *Inorg. Chem.* **2009**, *48*, 1281–1283; d) J. Boonmak, S. Youngme, N. Chaichit, G. A. van Albada, J. Reedijk, *Cryst. Growth Des.* **2009**, *9*, 3318–3326; e) Y.-H. Chung, H.-H. Wei, G.-H. Lee, Y. Wang, *Inorg. Chim. Acta* **1999**, *293*, 30–36.
- [4] a) M. Kato, T. Tanase, M. Mikuriya, *Inorg. Chem.* **2006**, *45*, 2925–2941; b) C. J. Boxwell, R. Bhalla, L. Cronin, S. S. Turner, P. H. Walton, *J. Chem. Soc., Dalton Trans.* **1998**, 2449–2450; c) J. Zhang, Y. Kang, J. Zhang, Z.-J. Li, Y.-Y. Qin, Y.-G. Yao, *Eur. J. Inorg. Chem.* **2006**, 2253–2258; d) M. S. E. Fallah, A. Escuer, R. Vicente, F. Badyine, X. Solans, M. Font-Bardia, *Inorg. Chem.* **2004**, *43*, 7218–7226.
- [5] a) J.-P. Zhao, B.-W. Hu, Q. Yang, T.-L. Hu, X.-H. Bu, *Inorg. Chem.* **2009**, *48*, 7111–7116; b) S. Wang, S. J. Trepanier, J.-C. Zheng, S. Pang, M. J. Wagner, *Inorg. Chem.* **1992**, *31*, 2118–2127; c) C. Lopez, R. Costa, F. Illas, C. d. Graaf, M. M. Turnbull, C. P. Landee, E. Espinosa, I. Mata, E. Molins, *Dalton Trans.* **2005**, 2322–2330.
- [6] a) Z. He, Z.-M. Wang, S. Gao, C.-H. Yan, *Inorg. Chem.* **2006**, *45*, 6694–6705; b) Y.-F. Zeng, J.-P. Zhao, B.-W. Hu, X. Hu, F.-C. Liu, J. Ribas, J. Ribas-Ari, X.-H. Bu, *Chem. Eur. J.* **2007**, *13*, 9924–9930; c) V. Tangoulis, D. Panagoulis, C. P. Raptopoulou, C. Dendrinou-Samar, *Dalton Trans.* **2008**, 1752–1760; d) L. K. Thompson, S. S. Tandon, F. Lloret, J. Cano, M. Julve, *Inorg. Chem.* **1997**, *36*, 3301–3306.
- [7] Y. Li, F.-K. Zheng, J.-P. Zou, W.-Q. Zou, H.-W. Ma, G.-C. Guo, C.-Z. Lu, J.-S. Huang, *Inorg. Chem. Commun.* **2007**, *10*, 787–792.
- [8] a) L.-P. Zhang, T. C. W. Mak, *Polyhedron* **2003**, *22*, 2787–2798; b) L.-P. Zhang, T. C. W. Mak, *J. Mol. Struct.* **2004**, *693*, 1–10; c) P.-R. Wei, D.-D. Wu, Z.-Y. Zhou, T. C. W. Mak, *Polyhedron* **1998**, *17*, 497–505; d) J.-G. Mao, T. C. W. Mak, H.-J. Zhang, J.-Z. Ni, S.-B. Wang, *J. Coord. Chem.* **1999**, *47*, 145–149.
- [9] a) J.-G. Mao, H.-J. Zhang, J.-Z. Ni, S.-B. Wang, T. C. W. Mak, *Polyhedron* **1999**, *18*, 1519–1525; b) M.-Y. Chow, Z.-Y. Zhou, T. C. W. Mak, *Inorg. Chem.* **1992**, *31*, 4900–4902; c) L. K. Thompson, S. S. Tandon, F. Lloret, J. Cano, M. Julve, *Inorg. Chem.* **1997**, *36*, 3301–3306.
- [10] Y. Li, J.-P. Zou, W.-Q. Zou, F.-K. Zheng, G.-C. Guo, C.-Z. Lu, J.-S. Huang, *Inorg. Chem. Commun.* **2007**, *10*, 1026–1030.
- [11] a) Y.-Q. Wang, J.-Y. Zhang, Q.-X. Jia, E.-Q. Gao, C.-M. Liu, *Inorg. Chem.* **2009**, *48*, 789–791; b) C.-Y. Tian, W.-W. Sun, Q.-X. Jia, H. Tian, E.-Q. Gao, *Dalton Trans.* **2009**, 1–5; c) Y. Ma, J.-Y. Zhang, A.-L. Cheng, Q. Sun, E.-Q. Gao, C.-M. Liu, *Inorg. Chem.* **2009**, *48*, 6142–6151; d) W.-W. Sun, C.-Y. Tian, X.-H. Jing, Y.-Q. Wang, E.-Q. Gao, *Chem. Commun.* **2009**, 4741–4743.
- [12] a) K. S. Murray, *Adv. Inorg. Chem.* **1996**, *43*, 261–358; b) G. Aromi, E. K. Brechin, *Struct. Bonding (Berlin)* **2006**, *122*, 1–67.
- [13] N. Lah, J. Koller, G. Giester, P. Segedin, I. Leban, *New J. Chem.* **2002**, *26*, 933–938.
- [14] R. G. Little, J. A. Moreland, D. B. W. Yawney, R. J. Doedens, *J. Am. Chem. Soc.* **1974**, *96*, 3834–3842.
- [15] a) R. W. Jotham, S. F. A. Kettle, *Inorg. Chim. Acta* **1970**, *4*, 145–149; b) Y.-f. Song, C. Massera, O. Roubeau, P. Gamez, A. M. M. Lanfredi, J. Reedijk, *Inorg. Chem.* **2004**, *43*, 6842–6847.
- [16] V. H. Crawford, H. W. Richardson, J. R. Wasson, D. J. Hodgson, W. E. Hatfield, *Inorg. Chem.* **1976**, *15*, 2107–2116.
- [17] a) P.-P. Liu, A.-L. Cheng, N. Liu, W.-W. Sun, E.-Q. Gao, *Chem. Mater.* **2007**, *19*, 2724–2726; b) S. Triki, J. C. Gómez-García, E. Ruiz, J. Sala-Pala, *Inorg. Chem.* **2005**, *44*, 5501–5508; c) S.-Q. Bai, E.-Q. Gao, Z. He, C.-J. Fanga, C.-H. Yan, *New J. Chem.* **2005**, *29*, 935–941.
- [18] a) O. Kahn, *Molecular Magnetism*, VCH Publishers, New York, **1993**; b) S. Ménage, S. E. Vitols, P. Bergerat, E. Codjovi, O. Kahn, J. J. Girerd, M. Guillot, X. Solans, T. Calvetll, *Inorg. Chem.* **1991**, *30*, 2666–2671; c) C. Golze, A. Alfonsov, R. Klingeler, B. Büchner, V. Kataev, C. Mennerich, H. H. Klaus, M. Goiran, J. M. Broto, H. Rakoto, S. Demeshko, G. Leibel, F. Meyer, *Phys. Rev. B* **2006**, *73*, 224403-1-8.
- [19] S. J. Loeb, J. Tiburcio, S. J. Vella, J. A. Wisner, *Org. Biomol. Chem.* **2006**, *4*, 667–680.
- [20] G. M. Sheldrick, *Program for Empirical Absorption Correction of Area Detector Data*, University of Göttingen, Germany, **1996**.
- [21] G. M. Sheldrick, *SHELXTL Version 5.1*, Bruker Analytical X-ray Instruments Inc., Madison, Wisconsin, USA, **1998**.
- [22] D. Lee, P.-L. Hung, B. Spingler, S. J. Lippard, *Inorg. Chem.* **2002**, *41*, 521–531.

Received: November 19, 2009

Published Online: February 2, 2010